Asian Journal of Chemistry; Vol. 37, No. 9 (2025), 2251-2257
ASIAN JOURNAL OF CHEMISTRY
https://doi.org/10.14233/ajchem.2025.34247

Paspalum vaginatum Extract-Mediated Synthesis of ZnO Nanoparticles and Assessment of their Photocatalytic and Antibacterial Activities

HENRY U. ANUFORO[1,*], PRISCILLA N. ABARA[1], NNEAMAKA A. CHIEGBOKA[1], ANGELA C. UDEBUANI[2], OLUSOLA O. IBEH[3], JUSTIN C. NNOKWE[1], LAWRENCIA A. ADJEROH[1] and TOOCHUKWU E. OGBULIE[2]

[1]Department of Biology, School of Biological Sciences, Federal University of Technology, PMB 1526, Owerri, Nigeria
[2]Department of Biotechnology, School of Biological Sciences, Federal University of Technology, PMB 1526, Owerri, Nigeria
[3]Department of Forensic Science, School of Biological Sciences, Federal University of Technology, PMB 1526, Owerri, Nigeria

*Corresponding author: E-mail: henry.anuforo@futo.edu.ng

Received: 13 June 2025 *Accepted*: 14 August 2025 *Published online*: 30 August 2025 AJC-22106

Phytochemical screening of *Paspalum vaginatum* extract was conducted prior to its use in the biosynthesis of zinc oxide nanoparticles (ZnO NPs), which were subsequently characterized using several analytical techniques. Results revealed high concentrations of carbohydrates, alkaloids, amino acids and proteins, phenolic compounds and flavonoids in the extract. UV-visible spectrum of biosynthesized ZnO NPs showed maximum absorbance at 307 nm. The X-ray diffraction (XRD) pattern confirmed a hexagonal wurtzite crystalline structure, with an estimated crystallite size of 23.6 nm. Resulting transmission electron micrograph (TEM) revealed spherical-shaped ZnO NPs, with average size of 3.96 ± 2.4 nm. Antibacterial analysis against isolates of *Salmonella typhi* and *Staphylococcus aureus* produced 11.33 ± 7.2 mm and 16 ± 3.2 mm zones of inhibition at 53.3 µg/mL, respectively. Also, percentage degradation of methyl orange dye solution was 13.16 ± 1.8%, 28.84 ± 0.6% and 32.74 ± 3.1% using 1.72 mg/mL of ZnO NPs, after 1, 2 and 3 h of solar irradiation. Thus, *P. vaginatum* extract is suitable for biogenic synthesis of ZnO NPs which possess appreciable bioactivities.

Keywords: ZnO Nanoparticles, *Paspalum vaginatum*, Photocatalytic activity, Antibacterial activity.

INTRODUCTION

In recent years, nanotechnology has gained increasing recognition for its potential to enhance products across diverse fields, including cosmetics, healthcare, diagnostics, catalysis, optics, food industry and the treatment of various medical infections [1,2]. Nanoparticles, as direct products of nanotechnology, exhibit superior biological and physico-chemical properties compared to their bulk counterparts, primarily due to their small sizes (1–100 nm) and significantly larger surface-to-volume ratios [3-5]. This accounts for their increased surface reactivity [1,6].

There are different methods of synthesizing different nanoparticles, including physical, biological and chemical methods, with diverse sizes and morphologies [7]. However, the biological method, which incorporates extracts of plants, microorganisms, *etc*. has been recognized to be simpler, more eco-friendly, cost-effective and sustainable [8]. This bottom-up approach entails the assembly of discrete smaller sized atoms and compounds, in the precursor, into larger final nano-sized products [9]. Recently, this method has increasingly been applied in eco-friendly synthesis of nanoparticles of different metals and their metal oxides [1].

Zinc oxide nanoparticles (ZnO NPs), unlike other known metal oxide nanoparticles, have shown very interesting features, which made them useful in optics, magnetism, piezoelectricity and gas sensing. Moreover, they also possess strong adsorption ability, high catalytic potentials and are useful in manufacturing sunscreens [2,10]. ZnO NPs are used as materials for food preservation, packaging, coating, biological tagging, cytotoxic applications and in agriculture [2,11]. Several researchers have used many extracts of plants, such as leaf of *Cymbopogon citratus* [1], peels of *Citrus sinensis*, *Citrus limon* and *Citrus tangerine* [12], strawberry waste extract [2], leaf extract of *Ocimum lamifolium* [13] for the biosynthesis of nanoparticles. Reports have attributed this to their possession of different bioactive substances including flavonoids, phenols, terpenoids, proteins, alkaloids, carbohydrates, enzymes and

vitamins, in plant extracts. These bioactive substances, in place of chemical reagents, reduce and cap metal ion to lower valence state [14,15]. The biosynthesis of ZnO NPs occurs in three main stages *viz*. activation, where plant metabolites reduce zinc ions to atoms; nucleation and growth through Ostwald ripening, involving the aggregation of smaller particles into larger ones. It encompasses heterogeneous nucleation, growth, with further reduction of zinc ions and leads to increase in thermodynamic stability of resulting nanoparticles. Lastly is the termination stage, at which nanoparticle shapes are finally determined, coupled to formation of well-dispersed, stable ZnO nanoparticles, after oxidation [1].

Although previous studies have reported successful nanoparticles synthesis using different plant extracts, many of them involved either medicinal plants or plants relevant in maintaining food security. Thus, increased dependence on such plants for biosynthesis of nanoparticles may result in their overexploitation and may render the biological method of nanoparticles synthesis unsustainable. This calls for diversification of sources of plant extracts. The present study used leaf extract of *Paspalum vaginatum* to biosynthesize ZnO nanoparticles and their antibacterial, as well as photocatalytic activities were investigated. This is geared toward the sustainability of biosynthesis of nanoparticles.

EXPERIMENTAL

All chemicals and reagents used were purchased from reliable, commercial suppliers and used without further purification.

Processing of plant extract: *Paspalum vaginatum* (seashore paspalum) leaves, used in this study were harvested from the Federal University of Technology, Owerri (FUTO), Nigeria. Collected samples were identified at the Department of Forestry and Wildlife Technology, FUTO and assigned the voucher no. FUTO/FWT/ERB/2024/108. They were processed into aqueous extract, in line with Akujobi *et al*. [16] method, with slight variations. First, the leaf samples were thoroughly sorted, washed under running water and then sun-dried to constant weight. This was followed by pulverizing them into powders, before storage in clean airtight containers, until use. Extract preparation was undertaken by weighing 107 g of ground sample into 2000 mL conical flask, containing 1500 mL of distilled water. It was boiled for 20 min, cooled and filtered with filter paper (Whatman No. 1). The concentration of obtained filtrate was determined in triplicates as described by Mahamadi & Wunganayi [17]. The filtrate was preserved at 4 ºC until further use.

Phytochemical screening of *P. vaginatum*: The leaf sample was qualitatively analyzed for the presence of phytochemicals as follow:

Phlorobatannins: Presence of phlorobatannins in leaf of *P. vaginatum* was analyzed following the method of Ejikeme *et al*. [18]. Weighed 0.3 g of leaf sample was added into 3 mL of distilled water in a beaker. Following 20 min of extraction, 10 mL of extract was mixed and boiled with 5 mL of 1% aqueous HCl. Positive test was confirmed by production of red precipitate.

Alkaloids: Presence of alkaloids was analyzed by adding 1 mL of Wagner's reagent to the side of slanted test tube containing 3 mL of *P. vaginatum* extract. Positive result was confirmed by formation of reddish-brown precipitate [18].

Saponin: Distilled water (3 mL) was pipetted into a test tube containing 0.3 g of ground leaf sample. It was boiled for 10 min in water bath and filtered using filter paper (Whatman No 1). Then resulting filtrate (1 mL) and distilled water (5 mL) were vigorously mixed. Positive test was confirmed by observation of stable persistent froth, as well as formation of emulsion on adding 0.5 mL of olive oil [18].

Carbohydrates: By adding 2 mL of Benedict's reagent into 2 mL of filtrate and boiling the mixture in water bath, for 2 min. Positive test for sugar was established by formation of precipitate with distinctive colouration [19].

Tannins: Few drops of 5% $FeCl_3$ solution was added into 1 mL of the plant extract. Positive test for catecholic tannins was confirmed by development of greenish-black colour; appearance of blue colour indicated positive test for gallic tannins; while formation of greenish-brown colour revealed positive test for condensed tannins [18].

Sterols and triterpenoids: Following the procedure of Ejikeme *et al*. [18], presence of sterols and triterpenoids was tested by adding 3 g of leaf sample into a beaker, containing 30 mL of distilled water and decocting for 20 min. Then a mixture of 3 mL conc. H_2SO_4 and 2 mL $CHCl_3$ was pipetted into 5 mL of the extract, to form a layer. Positive test for sterols was confirmed by observation of red coloured lower layer, while yellow coloured layer proved the presence of triterpenoids.

Mucilages and gums: In this test, 10 mL of aqueous extract was constantly stirred with 25 mL of absolute alcohol, before filtering. Positive test was confirmed by drying resulting precipitate in air, followed by its examination for swelling [18].

Flavonoids: Few drops of NaOH solution were used to treat a 3 mL of extract. Positive test was shown by change of intense yellow colour of the solution to colourless, when dilute HCl acid was added [20].

Amino acids and proteins: Distilled water (10 mL) was added into 5 g of plant extract and then decocted for 20 min, before filtration. Then 0.5 mL of Million's reagent was mixed with 2 mL of filtrate. Positive test for proteins was confirmed by formation of white precipitate [19].

Oils and fats: Test for fixed oil and fat was tested by pressing 1 mL of extract amid two filter papers. Positive test was confirmed by observation of oil stain on the paper [21].

Phenolic compounds: Three drops of 10% solution of lead acetate were mixed with 2 mL of plant extract. Positive test was confirmed by appearance of white precipitate [18].

Anthraquinone glycosides: Plant extract (3 mL) was mixed with 2 mL of dilute H_2SO_4, then boiled and filtered. On cooling, equal volumes of filtrate and chloroform were mixed. After separating the organic layer, ammonia was added. Positive test was confirmed by the change of ammonical layer to pink or red [18].

Cardiac glycoside: This test was done by mixing of glacial acetic acid, 2 mL of plant extract, conc. H_2SO_4 and 0.5 mL of 5% $FeCl_3$. Positive test was confirmed by develop-

ment of reddish-brown colouration at interface of the two layers [18].

Biosynthesis of ZnO NPs: Biosynthesis of ZnO NPs was performed according to the reported method [22,23] with some modifications. Initially, the temperatures of 10 mL *P. vaginatum* extract and 90 mL of 0.05 M of precursor $Zn(NO_3)_2 \cdot 6H_2O$ solution were increased to 80 ºC in a water bath. Then the pH of extract was adjusted to 10 by dropwise addition of 0.1 M NaOH solution. Biosynthesis was done by gradual addition of the precursor solution into the extract, with constant stirring of the mixture at 80 ºC for 30 min. Afterward, the reacting mixture was kept at 25-28 ºC for 24 h for completion of reaction. Visual observation of changes in colour of reacting mixture, during biosynthesis, was made. The suspension was then centrifuged for 30 min at 5000 rpm and then washed three times with distilled water.

Characterization: The biosynthesized ZnO NPs were characterized by determining their UV-visible absorbance spectrum, in 2 mL quartz cuvette, at a resolution of 1 nm within 200–800 nm range of wavelength. Presence of functional groups in synthesized ZnO NPs was determined by Fourier transform infrared (FTIR) spectroscopy using KBr pallets discs in the 4000-500 cm^{-1} range. The crystalline nature, including phase texture, composition and crystal structure or orientation of synthesized ZnO NPs, were determined using X-ray diffractometer (X'pert Pananalytical) instrument, set at 30 mA and 40 kV, using Cu*K*α radiation. The size of the synthesized ZnO NPs crystals was predicted according to Scherrer's formula:

$$L = \frac{k\lambda}{\beta \cos\theta} \quad (1)$$

where L is ZnO NPs crystalline size, θ is the diffraction angle (36.42), K = 0.94 (Scherrer's constant), β is the full width at half maximum (FWHM) of highest diffraction peak (detected to be 0.37) and λ refers to wavelength of X-ray (1.54178 Å) [24]. The size and morphology of biosynthesized ZnO NPs were carried out through transmission electron microscopy (JEOL 200CX) and resulting photomicrograph was analyzed using ImageJ software. The size distribution of nanoparticles in a solution was determined using Malvern Zen 3600 instrument [25].

Antibacterial activity: The antibacterial potential of the biosynthesized ZnO NPs was studied against clinical isolates of *Salmonella typhi* and *Staphylococcus aureus*, collected from the Diagnosis section of the FUTO Teaching Hospital, Owerri, Nigeria. After identification using specific differential media, antibacterial analysis was done in duplicates, using the agar well diffusion method [26], with some modifications. This was done by separately inoculating a loopful of each bacterial culture into 5 mL of nutrient broth and incubating for 24 h, at 37 ºC, to revive the cultures. Each of the isolates was standardized by adjusting the turbidity to match 0.5 McFarland solution (~10^8 cfu/mL). Then standardized test inoculum (0.1 mL) was aseptically spread onto prepared Mueller-Hinton (MH) agar plates.

Then different concentrations of biosynthesized ZnO NPs, including 53.3 µg/mL, 26.7 µg/mL and 13.3 µg/mL, were separately prepared. Wells were created into the Mueller-Hinton (MH) agar plates using sterilized borers. Afterward, few drops of each concentration of ZnO NPs were transferred into appropriately labelled wells and the plates were allowed for nanoparticles to permeate the media. Ciprofloxacin and distilled water served as positive and negative controls, respectively. Plates were incubated at 37 ºC for 24 h, before diameter of growth inhibition zones were measured for each test bacterium [27].

Photocatalytic activity: The photocatalytic potential of biosynthesized ZnO NPs was analyzed as described by Biswas & Mulaba-Bafubiandi [28], with some modifications. It was undertaken under solar light, using aqueous solution of methyl orange (MO) dye. Initially, 1 mL of each of 53.3 mg/mL, 26.7 mg/mL and 13.3 mg/mL of biosynthesized ZnO NPs were separately added into 30 mL of 0.5 mg/L of the dye solution. The mixtures were continuously stirred for 30 min in the dark, to ensure uniformity, thus giving final ZnO NPs concentrations of 1.72 mg/mL, 0.86 mg/mL and 0.43 mg/mL. Subsequently, the mixtures were placed under the sun, between 12 pm and 4 pm on sunny days. After stirring, aliquot of treated sample was carefully withdrawn at intervals of 0, 60, 120 and 180 min and then centrifuged for 10 min, at 4000 rpm, to remove photocatalysts. Analysis of photocatalytic breakdown of the dye was done by determining the UV visible absorbance at 464 nm [29]. Control experiment was also set up in duplicates without addition of ZnO NPs. The percentage dye degradation over period of exposure was computed with eqn. 2:

$$\text{Dye degradation (\%)} = \frac{C_o - C_t}{C_o} \times 100 \quad (2)$$

where C_o refers to the concentration of dye before treatment and C_t is the concentration of dye after t min of treatment.

Statistical analysis: The averages and standard deviations of all results arising from these studies were statistically determined appropriate tools in Microsoft Excel 2010 and Minitab 17 software.

RESULTS AND DISCUSSION

Average pH of the aqueous extract of *P. vaginatum* leaf sample was 6.5 ± 0.9 and the average concentration was 7.33 ± 1.89 mg/mL.

Phytochemical constituents of *P. vaginatum* extract: Result obtained indicated that the *P. vaginatum* aqueous leaf extract contained high quantities of alkaloids, proteins and amino acids, carbohydrates, phenolic compounds and flavonoids, are present. Tannins, oils and fats were only moderately present, whereas saponin, phlorobatannins, triterpenoids and cardiac glycosides were just slightly present in the extract. However, anthraquinone glycosides, sterols, gums and mucilages were absent in the extract as shown in Table-1. As suggested, the reduction and capping of metal ions into nano-sized particles have been attributed to these metabolites [30].

Characteristics: The average concentration of ZnO NPs biosynthesized using 10 mL aqueous leaf extract of *P. vaginatum* of pH 10 and 90 mL of 0.05 M $Zn(NO_3)_2 \cdot 6H_2O$, at 80 ºC for 24 h, was 2.53 ± 0.1 mg/mL, while the average size was 36.99 ± 0.7 nm. During biosynthesis, it was observed that the colour of extract changed from brown solution to dark-brown precipitate. Colour change observed in this study has

TABLE-1
PHYTOCHEMICAL CONSTITUENTS OF
P. vaginatum AQUEOUS LEAF EXTRACT

Phytochemical	Inference
Phlorobatannins	+
Saponin	+
Alkaloids	+++
Carbohydrate	+++
Sterols	–
Triterpenoids	+
Tannins (catecholic tannins)	++
Gums and mucilage	–
Amino acids and proteins	+++
Flavonoids	+++
Oil and fats	++
Anthraquinone glycosides	–
Phenolic compounds	+++
Cardiac glycoside	+

+++ implies high concentration; ++ implies moderate concentration; + implies slight concentration; and – means absent.

been corroborated by another study in which visual observation of colour change, from pale red to light brownish precipitate, when *C. citratus* ALE extract and zinc acetate were reacted, demonstrated the biosynthesis of ZnO NPs [1].

The absorbance spectrum obtained from UV-visible characterization of biosynthesized ZnO NPs (Fig. 1), showed that its absorbance ranged from 293 nm to 336 nm, with a peak of absorbance recorded at 307 nm. This implies that the absorbance of the biosynthesized ZnO NPs lies within the UV region. In a related study, report indicated that absorbance spectrum of synthesized ZnO NPs had a peak at 311 nm, which characterizes ZnO NPs, in view of its surface plasma resonance (SPR) [2]. Furthermore, ZnO NPs, prepared in another study, was reported to show absorption spectrum within 263-339 nm [13].

The FTIR spectrum (Fig. 2) revealed presence of diverse peaks. The appearances of peaks, functional groups and compounds present on the synthesized ZnO NPs were determined and are as shown in Table-2. The FTIR spectrum of ZnO NPs produced peak at about 3394 cm^{-1}, corresponding to bending and stretching vibrations of H–O–H and –OH functional groups of adsorbed water molecules. Another band appeared at 1644-1411 cm^{-1} representing the aromatic rings stretching and vibration, whereas band at 899 cm^{-1} indicated the C–H stretching [13]. The bands at 1418, 1559, 1629 and 2345 cm^{-1}

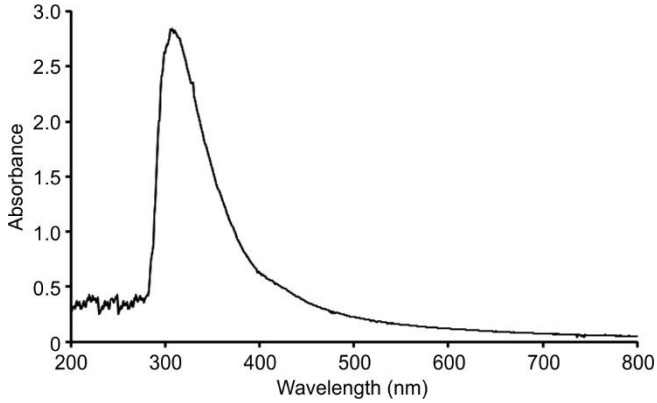

Fig. 1. Absorbance spectrum for ZnO NPs biosynthesized using aqueous extract of *P. vaginatum*

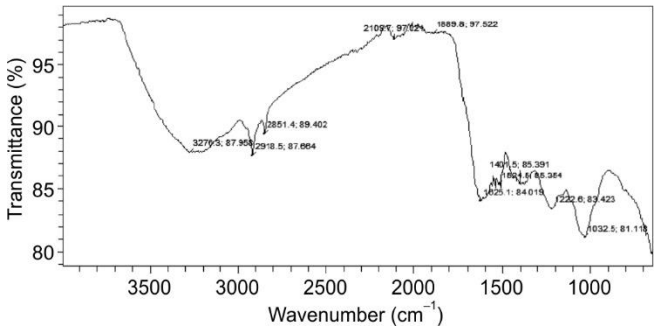

Fig. 2. FTIR spectrum of ZnO NPs biosynthesized with aqueous extract of *P. vaginatum*

corresponded to fused C=O, C=C and C-H stretching and vibrations of ketones and alkane respectively [2].

Results of DLS analysis in the present study, revealed that mean size of synthesized pure ZnO NPs was 35.34 ± 1.64 nm, with polydisperity index of 0.6335. According to Badran [31], when the polydispersity index values is less than 0.3, the nanoparticles preparation is said to be monodispersed. Consequently, the ZnO NPs biosynthesized in this study were polydispersed, as proven by the results of TEM. Similar study by Abdelbaky *et al.* [1] had also demonstrated that prepared ZnO NPs had mean size of approximately 28 nm, with polydispersity index (PDI) of 0.198.

The XRD pattern indicated that biosynthesized ZnO NPs were crystalline in structure. Eleven peaks (Fig. 3) with 2θ of 4.62º, 9.02º, 13.46º, 31.92º, 33.28º, 34.62º, 36.44º, 47.64º, 56.84º, 63.02º and 68.16º. The peaks at 2θ values and their

TABLE-2
DESCRIPTION OF PEAKS IN FTIR SPECTRUM OF ZnO NPs

Absorbance peak (cm^{-1})	Appearance	Functional group	Compound present
3276.3	Strong	O–H stretching; C–H stretching	Alcohol (intermolecular bonded); Alkyne
2918.5	Strong	N–H stretching	Amine salt
2851.4	Strong	C–H stretching	Alkane
2109.7	Weak	C≡C stretching	Alkyne
1889.8	Weak	C–H bending	Aromatic compound
1625.1	Strong	C=C stretching; N-H bending	Conjugated alkene; Amine
1524.5	Strong	N-O stretching	Nitro compound
1401.5	Strong	S=O stretching	Sulfonyl chloride
1222.6	Strong	C-O stretching	Alkyl aryl ether
1032.5	Strong	S=O stretching	Sulfoxide

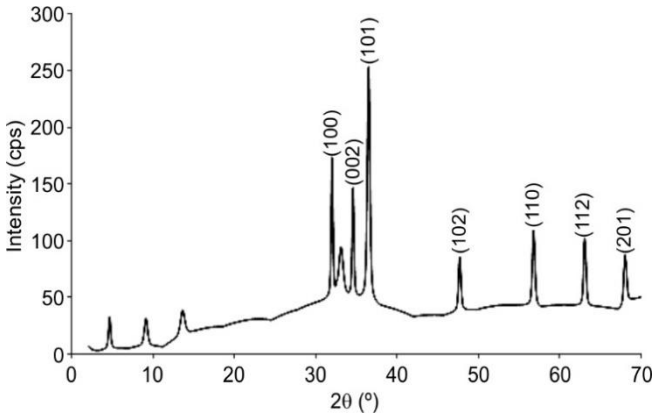

Fig. 3. XRD spectrum of ZnO NPs biosynthesized with *P. vaginatum* extract

corresponding orientation planes, are 31.92º (100), 34.62º (002), 36.44º (101), 47.64º (102), 56.84º (110), 63.3º (200) and 68.16º (112). The XRD patterns proved that biosynthesized ZnO NPs crystallize had hexagonal wurtzite structure. The high crystallinity of the biosynthesized ZnO NPs is shown by the sharp and intense peaks formed. The estimated crystalline size was 23.6 nm, with the 2θ peak positions specified with the JCPDS No. 04-005-5076. These findings were corroborated by previous studies. Peerakiatkhajohn *et al.* [32] had reported XRD pattern with peaks at 31.84° (100), 34.54º (002), 36.36º (101), 47.66º (102), 56.74º (110), 62.92º (103), 66.56º (200), 67.98º (112) and 69.22º (201), with hexagonal, wurtzite structure ZnO NPs, having JCPDS No.: 00-036-1451. Similarly, the mean crystallite size of ZnO NPs biosynthesized by Tilahun *et al.* [13] was estimated to be 21.8 nm. Also, the XRD patterns of ZnO NPs biosynthesized using extract of *Citrus citratus*, indicated 2θ values at 31.85º, 34.55º, 36.35º, 47.69º, 56.75º, 63.09º, 66.56º, 68.17º, 69.29º, 72.87º and 77.21º. Another report showed that crystallite size of biosynthesized ZnO NPs was 19.01 nm, with the characteristic ZnO wurtzite structure. Its 2θ values were at 31.9º, 34.56º, 36.42º, 47.62º, 56.8º, 63.04º and 68.14º, which was indexed as JCPDS data card No. 36–1451 [2].

The resulting TEM micrograph of biosynthesized ZnO NPs (Fig. 4), at 100 nm resolution, revealed the formation of non-uniform sizes, which ranged from 0.52 nm to 8.32 nm, with an average of 3.96 ± 2.4 nm. They were mainly spherical in shape, polydispersed and without agglomeration. The characteristic three parts of nanoparticles, including the light, darkest and dark part were visibly observable on the TEM micrograph. A related study had similarly reported that micrograph of ZnO NPs showed the spherical mesoparticles with 6.5 nm average size [13]. Another study stated that TEM micrograph indicated that their synthesized ZnO NPs were spherical and on nanoscale, with 50 nm mean size [2].

Antibacterial activities: The zones of inhibition of *S. typhi* and *S. aureus* by ZnO NPs biosynthesized using leaf extract of *P. vaginatum* were 11.33 ± 7.2 mm and 16 ± 3.2 mm at 53.3 µg/mL; 4.0 ± 2.2 mm and 6.7 ± 2.1 mm at 26.7 µg/mL; and 0.0 ± 0.0 mm and 0.0 ± 0.0 mm at 13.3 µg/mL respectively. However, ciprofloxacin exhibited the highest ZoI of 25.1 mm, whereas no visible zone of inhibition was observed for distilled water (Fig. 5). From these results, it is observable that *S. aureus* showed higher sensitivity to both ZnO NPs and

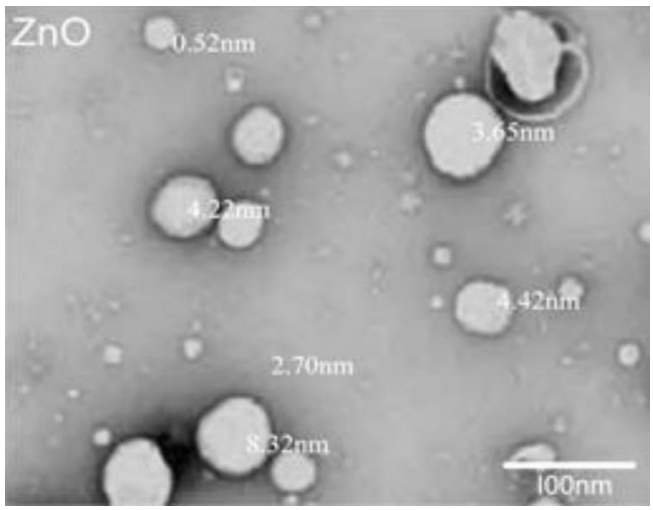

Fig. 4. Transmission electron micrograph of ZnO NPs biosynthesized with *P. vaginatum* extract, at 100 nm resolution

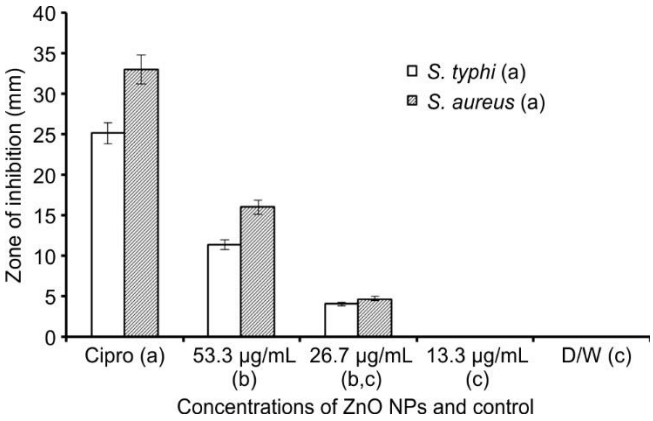

Fig. 5. Zones of inhibition of clinical isolates of *S. typhi* and *S. aureus* by different concentrations of biosynthesized ZnO NPs. Samples with similar letters, in parenthesis, are not significantly different

ciprofloxacin, than *S. typhi*. Statistical analysis ($\alpha = 0.05$) of the results proved that only the ZoI recorded at 53.3 µg/mL was not significantly lower than ZoI exhibited by ciprofloxacin (positive control). Higher sensitivity to ZnO NPs was observed in *S. aureus* than in *S. typhi*, as also observed for ciprofloxacin. However, the variation did not make them significantly different ($\alpha = 0.05$) from each other in their sensitivities.

Effective antibacterial activity of ZnO NPs had been reported in several studies. A study showed that *S. aureus* isolate was more sensitive to ZnO NPs, than *P. aeruginosa* and *E. coli* isolates, at all concentrations studied. At 100 µg/mL, it reportedly showed appreciably high zones of inhibition against the isolates, though ampicillin, used as the positive control, exhibited higher activity than ZnO NPs [13]. Also, Abdelbaky *et al.* [1] indicated that the log of colony forming units (CFU) of *S. aureus* treated with green synthesized ZnO NPs reduced across the concentrations studied, unlike in the control sample. Thus, the highest percentage bacterial growth inhibition for *S. aureus*, recorded at 200 µg/mL concentration of ZnO NPs, was 94.66%; which reduced to 88.50% at 100 µg/mL concentration, 77.35% at 50 µg/mL and 65.74% at 25 µg/mL concentrations, compared to 0.0% in negative control and 40.20% with amoxicillin.

The higher sensitivity recorded in *S. aureus* than *S. typhi* in this study is attributable to the differences in their cell wall structure and composition. While *S. aureus* is Gram-positive, *S. typhi* is Gram-negative. Lallo da Silva *et al*. [33] had stated that Gram-negative nature of bacterial cells makes it easier for nanoparticles to enter bacterial cell wall and inhibit their growth or kill the cells. Conversely, peptidoglycan layer surrounding Gram-positive bacteria could promote ZnO NPs attack inside the cell wall by limiting their exit. Furthermore, lipopolysaccharides found in Gram-negative bacteria are capable of exerting a counterattack on ZnO NPs, which may reduce their activity.

Photocatalysis of dye wastewater: Using 1.72 mg/mL concentration of ZnO NPs biosynthesized with leaf extract of *P. vaginatum*, in this study as photocatalyst, the recorded percentage degradation of MO dye solution was 13.16 ± 1.8% after 1 h, 28.84 ± 0.6% after 2 h and 32.74 ± 3.1% after 3 h of exposure to solar light. The percentage degradation declined to 9.14 ± 1.5%, 14.92 ± 0.2% and 18.44 ± 1.4% after 1 h, 2 h, 3 h of exposure, respectively, when concentration of photocatalyst reduced to 0.86 mg/mL. Further reduction of concentration of ZnO NPs to 0.43 mg/mL also reduced the percentages of degradation to 5.78 ± 1.4%, 6.27 ± 0.0% and 6.6 ± 0.3% after 1 h, 2 h and 3 h of exposure, respectively. These percentages were comparably higher than 4.67 ± 2.2% recorded in control samples after 1 h, 6.41 ± 1.1% after 2 h and 6.63 ± 1.0% after 3 h of exposure to solar light (Fig. 6). From statistical analysis, only the percentage degradation recorded in samples treated with 1.72 mg/mL of ZnO NPs was significantly higher than that of control samples. However, it was similar to the result recorded at 0.86 mg/mL of ZnO NPs. Statistical modelling of the results showed that photocatalytic activity of 1.72 mg/mL biosynthesized ZnO NPs on 0.5 mg/mL methyl orange dye solution, is best described by the polynomial equation; $y = -5.8873x^2 + 33.339x - 14.292$, with $R^2 = 1$; where x is time (h) while y is percentage degradation of methyl orange dye.

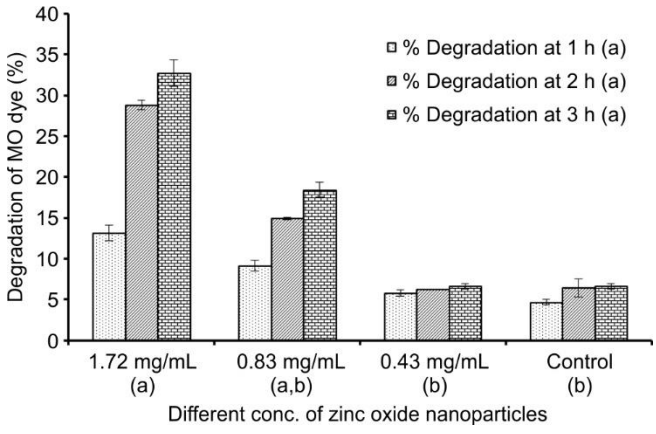

Fig. 6. Percentage degradation of MO dye using different concentrations of ZnO NP photocatalyst, over 3 h. Samples with different lower case letters in parenthesis, are significantly different

Findings similar to those of the present study had been reported. In their study, Peerakiatkhajohn *et al*. [32] reported that the highest methyl orange removal efficiency of 80%, was recorded in ZnO NPs calcined at 200 ºC, after 4 h of irradiation under ultraviolet light. Similarly, another study showed that highest percentage methyl orange dye degradation by ZnO NPs was 88%, at pH 8, under the UV light irradiation [34]. These values are evidently higher than those of the present study since their samples were irradiated under UV light, unlike in the present study that used visible light. This finding aligns with the result of UV visible absorbance, which revealed that the absorbance peak of biosynthesized ZnO NPs occurred at 307 nm, which lies within the ultraviolet region.

Conversely, Peerakiatkhajohn *et al*. [32] reported that under visible light irradiation of methyl orange dye solution, the degradation efficiency of ZnO photocatalysts recorded after 40 min was 5%. Thus, they concluded that irradiation of ZnO photocatalysts under UV light produces higher degradation efficiency than under visible light irradiation. This observation is attributable to the large bandgap of ZnO NPs, which limits its excitation to within the UV light region. When irradiated with visible light, the pathway of ZnO degradation is similar to production of radicals *via* charge migration, which degrades dye molecules [32]. Usually, at the onset of photocatalysis, the degradation rates are faster due to the availability of numerous active sites on ZnO NPs. After certain duration, equilibrium will be attained, thereby reducing the rate of degradation. This is attributed to repulsion between dye particles and catalyst surface [34].

Conclusion

In order to further diversify the sources of plant extracts for use in biosynthesis of nanoparticles, *Paspalum vaginatum* leaf extract was adopted in this study. The result obtained showed that *P. vaginatum* aqueous leaf extract contains necessary biomolecules and is useful in ZnO NPs biosynthesis. From the results of various characterization techniques, biosynthesized ZnO NPs satisfied necessary characteristics of ZnO NPs. Result of analysis proved that synthesized ZnO NPs produced appreciable antibacterial property against *S. typhi* and *S. aureus*. Also, the ZnO NPs showed good photocatalytic degradation potentials on methyl orange dye wastewater, under solar irradiation. There is a need to further optimize the effects of relevant physico-chemical factors on the property of resulting ZnO NPs

ACKNOWLEDGEMENTS

The authors are grateful to the Heads of Departments of Biotechnology, Biology and Microbiology, Federal University of Technology, Owerri, Nigeria, for providing the necessary research facilities.

CONFLICT OF INTEREST

The authors declare that there is no conflict of interests regarding the publication of this article.

REFERENCES

1. A.S. Abdelbaky, A.M.H.A. Mohamed, M. Sharaky, N.A. Mohamed and Y.M. Diab, *Chem. Biol. Technol. Agric.*, **10**, 63 (2023); https://doi.org/10.1186/s40538-023-00432-5
2. V. Khan, N. Malik, B. Singh, N.H. Ansari, M. Rehman and A. Yadav, *J. Umm Al-Qura Univ. Appl. Sci.*, **9**, 268 (2023); https://doi.org/10.1007/s43994-023-00038-5

3. H. Mohd Yusof, R. Mohamad, U.H. Zaidan and N.A. Abdul Rahman, *J. Anim. Sci. Biotechnol.*, **10**, 57 (2019); https://doi.org/10.1186/s40104-019-0368-z
4. S. Kaur and A. Roy, *Environ. Dev. Sustain.*, **23**, 9617 (2021); https://doi.org/10.1007/s10668-020-01078-1
5. X. Qiao, J. He, R. Yang, Y. Li, G. Chen, S. Xiao, B. Huang, Y. Yuan, Q. Sheng and T. Yue, *Processes*, **10**, 2576 (2022); https://doi.org/10.3390/pr10122576
6. R.S. Geonmonond, A.G.M.D.A. Silva and P.H.C. Camargo, *Academia Brasileira de Ciências*, **90,** (2018); https://doi.org/10.1590/0001-3765201820170561
7. D. Sharma, S. Kanchi and K. Bisetty, *Arab. J. Chem.*, **12**, 3576 (2019); https://doi.org/10.1016/j.arabjc.2015.11.002
8. R. Kumar Bachheti, A. Fikadu, A. Bachheti and A. Husen, *Saudi J. Biol. Sci.*, **27**, (2020); https://doi.org/10.1016/j.sjbs.2020.05.012
9. H. Kumar, K. Bhardwaj, R. Sharma, E. Nepovimova, K. Kuca, D.S. Dhanjal, R. Verma, P. Bhardwaj, S. Sharma and D. Kumar, *Molecules*, **25**, 2812 (2020); https://doi.org/10.3390/molecules25122812
10. X. Wang, J. Lu, M. Xu and B. Xing, *Environ. Sci. Technol.*, **42**, 7267 (2008); https://doi.org/10.1021/es8015414
11. J. Jiang, J. Pi and J. Cai, *Bioinorg. Chem. Appl.*, **2018**, 1 (2018); https://doi.org/10.1155/2018/1062562
12. M.C.D. Niluxsshun, K. Masilamani and U. Mathiventhan, *Bioinorg. Chem. Appl.*, **2021**, 1 (2021); https://doi.org/10.1155/2021/6695734
13. E. Tilahun, Y. Adimasu and Y. Dessie, *ACS Omega*, **8**, 27344 (2023); https://doi.org/10.1021/acsomega.3c02709
14. M. Can, *Rev. Chem. Eng.*, **36**, 859 (2020); https://doi.org/10.1515/revce-2018-0051
15. M.S. Samuel, M. Ravikumar, A. John J, E. Selvarajan, H. Patel, P.S. Chander, J. Soundarya, S. Vuppala, R. Balaji and N. Chandrasekar, *Catalysts*, **12**, 459 (2022); https://doi.org/10.3390/catal12050459
16. C.O. Akujobi, H.U. Anuforo, J.N. Okereke, C. Ibeh and C.J. Agbo, *An. Univ. Oradea Fasc. Biol.*, **27**, 21 (2020).
17. C. Mahamadi and T. Wunganayi, *Cogent Chem.*, **4**, 1538547 (2018); https://doi.org/10.1080/23312009.2018.1538547
18. C.M. Ejikeme, C.S. Ezeonu and A.N. Eboatu, *Eur. Sci. J.*, **10**, 18 (2014).
19. N. Raaman, Phytochemical Techniques, New India Publishing Agency: New Delhi, pp. 19-25 (2006).
20. M. Saxena, J. Saxena, R. Nema, D. Singh and A. Gupta, *J. Pharmacog. Phyto.*, **1**, 6 (2013).
21. K.S. Banu and L. Catherine, *Inter. J. Adv. Res. Chem. Sci.*, **2**, 4 (2015).
22. M.J. Haque, M.S. Bellah, M.R. Hassan and S. Rahman, *Nano Express*, **1**, 010007 (2020); https://doi.org/10.1088/2632-959X/ab7a43
23. H.U. Anuforo, T.E. Ogbulie, A.C. Udebuani and E.U. Ezeji, UMYU *J. Microbiol. Res.*, **8**, 74 (2023); https://doi.org/10.47430/ujmr.2382.009
24. O. Erdogan, M. Abbak, G.M. Demirbolat, F. Birtekocak, M. Aksel, S. Pasa and O. Cevik, *PLoS One*, **14**, e0216496 (2019); https://doi.org/10.1371/journal.pone.0216496
25. N. Amini, G. Amin and A.Z. Jafari, *Nanomed. Res. J.*, **2**, 57 (2017).
26. A. Chauhan, R. Verma, S. Kumari, A. Sharma, P. Shandilya, X. Li, K.M. Batoo, A. Imran, S. Kulshrestha and R. Kumar, *Sci. Rep.*, **10**, 7881 (2020); https://doi.org/10.1038/s41598-020-64419-0
27. H.F. Aritonang, H. Koleangan and A.D. Wuntu, *Int. J. Microbiol.*, **2019**, 3 (2019); https://doi.org/10.1155/2019/8642303
28. S. Biswas and A.F. Mulaba-Bafubiandi, *Nanosci. Nanotechnol.*, **7**, 045005 (2016); https://doi.org/10.1088/2043-6262/7/4/045005
29. S. Bhakya, S. Muthukrishnan, M. Sukumaran, M. Muthukumar, K.T. Senthil and M.V. Rao, *J. Bioremediat. Biodegrad.*, **6**, 312 (2015); https://doi.org/10.4172/2155-6199.1000312
30. Z. Sabouri, R. Kazemi Oskuee, S. Sabouri, S.S. Tabrizi Hafez Moghaddas, S. Samarghandian, H. Sajid Abdulabbas and M. Darroudi, *Ceram. Int.*, **49**, 20989 (2023); https://doi.org/10.1016/j.ceramint.2023.03.234
31. M. Badran, *Dig. J. Nanomater. Biostruct.*, **9**, 4 (2014).
32. P. Peerakiatkhajohn, T. Butburee, J.H. Sul, S. Thaweesak and J.H. Yun, *Nanomaterials*, **11**, 1059 (2021); https://doi.org/10.3390/nano11041059
33. B. Lallo da Silva, M.P. Abuçafy, E. Berbel Manaia, J.A. Oshiro Junior, B.G. Chiari-Andréo, R.C.L.R. Pietro and L.A. Chiavacci, *Int. J. Nanomedicine*, **14**, 9395 (2019); https://doi.org/10.2147/IJN.S216204
34. K.A. Isaia and V.S. Shrivastava, *Iranian J. Cat.*, **9**, 3 (2019).